GEOPHYSICAL RESEARCH LETTERS, VOL.34, L04602, DOI:10.1029/2006GL028243, 2007

Warming and oxygen-decrease of intermediate water in the northwestern North Pacific, originating from the Sea of Okhotsk, 1955–2004

Takuya Nakanowatari, Kay I. Ohshima, and Masaaki Wakatsuchi

Institute of Low Temperature Science, Hokkaido University,Sapporo, Japan

T. Nakanowatari, Institute of Low Temperature Science, Hokkaido University, Kita-19, Nishi-8, Kita-ku, Sapporo, 060-0819, Japan. (nakano@lowtem.hokudai.ac.jp)

On the basis of all available data, it is found that intermediate water temperature on the 26.8–27.4σ_θ isopycnals in the northwestern North Pacific has significantly increased during the past 50 years. The largest warming area exists in the western part of the Sea of Okhotsk with a 0.68°C/50-yr temperature increase observed at 27.0σ_θ. The warming in the Pacific is found over the Oyashio and Subarctic Current regions, where the Okhotsk water extends along the subarctic gyre. This suggests that the warming originates from the Sea of Okhotsk. The warming trend is also accompanied by the significant decreasing trend of dissolved oxygen content, suggesting the weakening of overturning in the northwestern North Pacific. We propose that these trends of the water mass property are caused by a decrease in dense shelf water production in the northwestern shelf of the Sea of Okhotsk, which is a sensitive area to the current global warming.

1. Introduction

It is known that North Pacific Intermediate Water (NPIW), characterized by a salinity minimum at $26.8\sigma_\theta$, is a major water mass at the intermediate level of the North Pacific [e.g., *Reid* 1965]. Several studies have suggested that the ventilation source of intermediate water in the North Pacific, including NPIW, is the Sea of Okhotsk [e.g., *Talley* 1991; *Warner et al.* 1996]. Over the northwestern shelf in the Sea of Okhotsk, a large amount of sea ice is produced due to severe winds from northeastern Eurasia in winter. The sea ice production leads to production of cold, oxygen-rich dense shelf water (DSW) with densities of up to $27.0\sigma_\theta$ [*Shcherbina et al.* 2003]. The DSW is transported southward into the intermediate layer of the deep Okhotsk basin in the southern Okhotsk Sea, and mixed with intermediate water coming from the North Pacific. This mixing forms the coldest, freshest and oxygen-richest water in the North Pacific in the density range of 26.8–$27.4\sigma_\theta$ [Talley 1991], which is called Okhotsk Sea Mode Water [*Yasuda et al.* 1997] or Okhotsk Sea Intermediate Water (OSIW) [*Itoh et al.* 2003]. The signal of OSIW extends downward to $27.4\sigma_\theta$ owing to diapycnal mixing caused by strong tidal currents around the Kuril Straits [*Wong et al.* 1998].

The OSIW outflows to the North Pacific through the Kuril Straits, mainly Bussol' Strait [Talley 1991], and then mixes with East Kamchatka Current Water, which flows southwestward along the northern Kuril Islands, forming the Oyashio water. The Oyashio water extends to the intermediate layer, flowing southwestward along the Kuril Island chain as the western boundary current of the subarctic gyre. The Oyashio water reaches the confluence of the subtropical and subarctic gyres, and then part of the Oyashio water

flows northeastward as the Subarctic Current (SAC), bounding the subarctic gyre on the south.

Recently, warming of intermediate water in the Sea of Okhotsk [*Hill et al.* 2003; *Itoh* 2006] and decreasing trends of dissolved oxygen content in intermediate water in the Oyashio [*Ono et al.* 2001] and western subarctic [*Andreev and Watanabe* 2002; Emerson et al. 2004] regions have been reported. However, the spatial extent and origin of these trends have not been clarified. In this paper, we examine the origin and spatial extent of the warming and oxygen decreasing trends of the intermediate water in these regions, by constructing gridded data set on isopycnal surfaces on the basis of all available data.

2. Data and Methods

Temperature, salinity and dissolved oxygen data were mainly taken from the World Ocean Database (WOD01) [*Conkright et al.* 2002]. In addition, we used observational data obtained by the Japan-Russia-United States international joint study of the Sea of Okhotsk from 1998 to 2004 and data archived by the Japan Oceanographic Data Center. We also used profiling float data obtained by the international Argo program from 2000 to 2004. The data from the recent international project in the Sea of Okhotsk and the Argo project enable us to discuss linear trend of intermediate water mass property until very recently. In this study, we focused on the density range 26.8–27.4σ_θ, on which the influence of deep water is small and to which winter convection does not directly reach in the open North Pacific [*Reid* 1965]. These isopycnal surfaces correspond to the intermediate layer influenced by ventilation from the Sea of Okhotsk [*Talley* 1991; *Warner et al.* 1998]. Data at discrete depths, mostly from bottle samples, were linearly interpolated to 1 m intervals, and then the values of potential temperature and dissolved oxygen were selected at 0.1σ_θ intervals. We applied a quality control, resulting in a data set of ∼63,000 stations at 27.0σ_θ in the northwestern North Pacific and the Sea of Okhotsk (35°–60°N, 135°E–140°W). For dissolved oxygen, the number of stations at 27.0σ_θ was about 30% of that for temperature.

Since the seasonal variation is negligible in the intermediate depths, annual mean climatologies of potential temperature and dissolved oxygen were calculated on a 0.25° latitude/longitude grid with a method similar to that by *Levitus and Boyer* [1994]. Since water mass properties in the Okhotsk Sea are distinctly different from those in the north-

western North Pacific, we produced their climatologies separately. For constructing the gridded data set, we used weighted averaging with a Gaussian window. We chose 150km as a half-width of the window and 75km as an e-folding scale to resolve regional features in the Sea of Okhotsk and the boundary current and fronts in the North Pacific. If the number of observations within the window of the center of a grid box was less than 5, that grid box was regarded as a no-data box. The derived climatologies on each isopycnal surface are quite similar to those of the North Pacific Hydrobase [*Macdonald et al.* 2001].

A gridded dataset of potential temperature anomalies on isopycnal surfaces was then prepared for the period 1955–2004, and one of dissolved oxygen for the period 1960–2004. First, we calculated anomalies of observed values as differences of the observed values from the produced climatologies. All the calculated anomalies were gridded by using simple averaging in a yearly $2.5^\circ \times 2.5^\circ$ grid box, taking account of the trade-off between spatial and temporal resolution. Neither spatial interpolation nor spatial smoothing was applied to the anomaly field.

3. Result

Figure 1 shows linear trend maps of intermediate water temperature on selected isopycnal surfaces for the last 50 years. Significant warming trends are observed in the northwestern North Pacific and the Sea of Okhotsk on all isopycnal surfaces. The warming trend in these regions is most prominent at density $27.0\sigma_\theta$, and the largest warming area exists in the western part (47.5°–55°N, 145°–147.5°E) of the Sea of Okhotsk with an average of 0.68°C/50-yr (Figure 1b). At $27.2\sigma_\theta$, the magnitude of the linear trend is smaller than that at $27.0\sigma_\theta$, though the spatial pattern is similar. On the other hand, the spatial pattern of the linear trend at $26.8\sigma_\theta$ is different from those at 27.0 and $27.2\sigma_\theta$; warming occurs in the western subarctic gyre, while cooling occurs over the region from the Kuroshio Extension to the south of the subpolar front (Figure 1a). The cooling trend is consistent with the fact that the significant cooling occurred down to the depth of 400m, which roughly corresponds to the $26.8\sigma_\theta$ surface, in the early 1980's [*Deser et al.* 1996].

The warming trend at $27.0\sigma_\theta$ seems to extend along the pathway of the OSIW. Climatology of the acceleration potential at $27.0\sigma_\theta$ (Figure 2) shows that the western subarctic gyre, which consists of the Oyashio and Subarctic Current (SAC), extends to the intermediate depth of $27.0\sigma_\theta$. A significant warming trend is observed in the Oyashio and SAC regions, but not in the East Kamchatska Current region, i.e., upstream of the Sea of Okhotsk. Since the intermediate water masses in the Oyashio and SAC regions are largely affected by the OSIW [*Yasuda* 1997], these results indicate that the warming trend in the northwestern North Pacific may be caused by advection of warmed OSIW.

Figure 3a shows the time series of temperature anomalies at 27.0σ_θ for the Sea of Okhotsk, Oyashio and SAC regions (Figure 2). A positive linear trend is the most significant feature in all three regions. Table 1 summarizes estimates of the linear trend of potential temperature from 26.8 to 27.4σ_θ for each region. The warming trend is most prominent at 26.9–27.0 σ_θ in the above three regions. At 27.0 σ_θ, the temperature has increased by 0.62 $\pm$0.18°C (significant at 99% confidence interval) in the Sea of Okhotsk during the past 50 years from 1955 through 2004, which is roughly consistent with the result reported by Itoh [2006]. The magnitude of the warming trend in the other two regions is about half of that.

We next examine the linear trend of dissolved oxygen content. For all three regions, significant negative trends are found (Figure 3b). The decrease of dissolved oxygen is most prominent at 26.9–27.0σ_θ, where the warming trend is most prominent (Table 1). At 27.0σ_θ, the linear trend in the Sea of Okhotsk is -0.58$\pm$0.34ml/l (significant at 95% confidence interval) for the past 45 years. The Oyashio and SAC regions have the value less than that for the Sea of Okhotsk. It is noted that the oxygen trend difference between the Sea of Okhotsk and Oyashio regions is relatively small when compared to the temperature trend difference between the two regions. Table 1 shows that the trends in temperature and dissolved oxygen are significant up to 27.4σ_θ for the Sea of Okhotsk and up to 27.2–27.3σ_θ for the Oyashio and SAC regions. Taking account of the effect of temperature variation on oxygen solubility, we examine trends of apparent oxygen utilization (AOU) of intermediate waters. The trend of AOU is approximately inversely proportional to that of dissolved oxygen, and both trends are equally statistically significant.

4. Discussion

It is shown that warming and oxygen-decreasing trends in the intermediate water are most prominent in the Sea of Okhotsk. Moreover, these trends appear to extend to the northwestern North Pacific along the pathway of the water mass originating from the Sea of Okhotsk. These facts suggest that trends in the northwestern North Pacific are due to preceding changes of water-mass properties in the Sea of Okhotsk. Intermediate water in the Sea of Okhotsk retains its cold and oxygen-rich properties by mixing with dense shelf water (DSW) associated with sea ice production in the coastal polynya of the northwestern shelf. The largest warming trend occurs in the western Sea of Okhotsk (Figure 1b), to which DSW is transported from the northwestern shelf [Fukamachi et al. 2004]. Therefore, we suppose that the main cause of the warming and oxygen-decreasing trends is the weakening of DSW production.

Although reliable estimation of DSW production is not yet available, there is some indirect evidence for a decrease trend in DSW production. Figure 4 shows the time series of surface air temperature anomaly in the cold season averaged over northeastern Eurasia, which is upwind of the Sea of Okhotsk; this air temperature can be an index of sea ice extent. This air temperature has increased considerably during the past 50 years (2.0 ± 1.4°C/50-yr, significant at 99% confidence level). Sea ice extent in the Sea of Okhotsk derived from satellite measurements, which is highly correlated with this air temperature (r=-0.61, significant at 95% confidence level), has decreased (-9.2%/27-yr) (Figure 4). Although satellite measurements have only been available since the 1970's, visual observations at Hokkaido coast, located on the southern boundary of sea ice extent

in the Sea of Okhotsk, show the decreasing trend of sea ice season length during the past 100 years [*Aota* 1999]. These trends of air temperature and sea ice season suggest that sea ice extent, accordingly sea ice production, have likely decreased during the past 50 years. During the current global warming, the surface air temperature anomaly in autumn and winter is particularly large over northeastern Eurasia [*Serreze et al.* 2000]. The DSW production area of the northwestern shelf in the Sea of Okhotsk is located where the winter monsoon from northeastern Eurasia directly transports cold air masses. Therefore, intermediate water in the Sea of Okhotsk which is ventilated through DSW may be sensitive to the global warming.

Several studies showed that most of the North Pacific has freshened in the upper layer recently [*Wong et al.* 1999; *Boyer et al.* 2005], which may be also related to the global warming. Also for the Sea of Okhotsk, *Hill et al.* [2003] reported a possibility of freshening in the upper layer. The freshening in the upper ocean would strengthen the stratification and thus weaken the ventilation or DSW production.

Recent studies suggest that OSIW has a significant role in material circulation of the intermediate layer in the North Pacific. *Hansell et al.* [2002] indicated that dissolved organic carbons in NPIW originate from the Sea of Okhotsk. *Nakatsuka et al.* [2004] showed that large amounts of dissolved and particulate organic carbons are exported from the highly productive northwestern shelf into the intermediate layer in the Sea of Okhotsk through the outflow of DSW. Moreover, recent observational data show that in the northwestern North Pacific, iron, which is an essential micronutrient for phytoplankton, may come from the intermediate water of the Sea of Okhotsk [*Nishioka* 2004]. The co-occurrence

of warming and decrease in dissolved oxygen concentration in the northwestern North Pacific, originating from the Sea of Okhotsk, implies that overturning in the northwestern North Pacific has weakened in the sense of material cycle. Therefore, such a trend has a possibility of substantial impacts on the material cycle and biological productivity in the North Pacific.

Acknowledgments. The Argo float data used in this study were collected and made freely available by the International Argo Project and the national programs that contributes to it. Part of the hydrographic data in the Okhotsk Sea were obtained under the cooperation with Far Eastern Regional Hydrometeorological Research Institute, Scripps Institute of Oceanography, and S. C. Riser of University of Washington. We wish to thank M. Itoh and K. Ono for data processing and anonymous reviewers for their constructive comments. Some figures are produced with the GrADS package.

References

Aota, M. (1999), Long-term tendencies of sea ice concentration and air temperature in the Okhotsk Sea coast of Hokkaido, *PICES Sci. Rep., 12*, 1-2, 1999.

Andreev, A. and S. Watanabe (2002), Temporal changes in dissolved oxygen of the intermediate water in the subarctic North Pacific, *Geophys. Res. Lett.*, *29*, 14, 10.1029/2002GL015021.

Boyer T. P., S. Levitus, J. I. Antonov, R. A. Locarnini, and H. E. Garcia (2005), Linear trends in salinity for the World Ocean, 1955–1998, *Geophys. Res. Lett.*, *32*, L01604, doi:10.1029/2004GL021791.

Conkright, M. E., et al. (2002), *World Ocean Database 2001*, vol. 1, *Introduction*, *NOAA Atlas NESDIS* 42 [CD-ROM], edited by S. Levitus, 167 pp., U.S. Govt. Print. Off., Washington, D.C.

Deser, C., M. A. Alexander, and M. S. Timlin (1996), Upper-ocean thermal variations in the North Pacific during 1970–1991, *J. Climate*, 9, 1840–1855.

Emerson, S., Y. W. Watanabe, T. Ono, and S. Mecking (2004), Temporal trends in apparent oxygen utilization in the upper pycnocline of the North Pacific: 1980–2000, *J. Oceanogr.*, 60, 139–147.

Fukamachi, Y., G. Mizuta, K. I. Ohshima, L. D. Talley, S. C. Riser, and M. Wakatsuchi (2004), Transport and modification processes of dense shelf water revealed by long-term moorings off Sakhalin in the Sea of Okhotsk, *J. Geophys. Res., 109*, C09S10, doi:10.1029/2003/JC001906.

Hansell, D. A., C. A. Carlson, and Y. Suzuki (2002), Dissolved organic carbon export with North Pacific Intermediate Water formation, *Global Biogeochem. Cycles, 16*(1), 1007, doi:10.1029/2000GB001361.

Hill, K. L., A. J. Weaver, H. J. Freeland, and A. Bychkov (2003), Evidence of change in the Sea of Okhotsk: implications for the North Pacific, *Atmosphere–Ocean, 41*, 49–63.

Itoh, M., K. I. Ohshima, and M. Wakatsuchi (2003), Distribution and formation of Okhotsk Sea Intermediate Water: an analysis of isopycnal climatology data, *J. Geophys. Res., 108*, 3258, doi:10.1029/2002JC001590.

Itoh, M. (2006), Warming of intermediate water in the Sea of Okhotsk since the 1950s, *J. Oceanogr., submitted*.

Jones P. D. (1994), Hemispheric surface air temperature variations: a reanalysis and an update to 1993, *J. Climate, 7*, 1794–1802.

Levitus, S., and T. Boyer (1994), *World Ocean Atlas 1994*, vol. 4, *Temperature*, NOAA Atlas NESDIS, vol. 4, 150pp., Natl. Oceanic and Atmos. Admin., Silver Spring, Md.

Macdonald A. M., T. Suga, and R. G. Curry (2001), An isppycnally averaged North Pacific climatology, *J. Atmos. Oceanic. Technol., 18*, 394–420.

Nakatsuka T., T. Toda, K. Kawamura, and M. Wakatsuchi (2004), Dissolved and particulate organic carbon in the Sea of Okhotsk: Transport from continental shelf to ocean interior, *J. Geophys. Res., 109*, C09S14, doi:10.1029/2003JC001909.

Nishioka J. (2004), Iron study in the Sea of Okhotsk: comparison to the subarctic Pacific, *Rep. on Amur–Okhotsk project*, 2, 103–109.

Ono, T., T. Midorikawa, Y. W. Watanabe, K. Tadokoro, and T. Saino (2001), Temporal increases of phosphate and apparent oxygen utilization in the surface waters of western subarctic Pacific from 1968 to 1998, *Geophys, Res. Lett., 28*, 3285–3288.

Rayner, N. A., D. E. Parker, E. B. Horton, C. K. Folland, L. V. Alexander, and D. P. Rowell (2003), Global analyses of sea surface temperature, sea ice, and night marine air temperature since the late nineteenth century, *J. Geophys. Res., 108*, D14,4407, doi:10.1029/2002JD002670.

Reid, J. L. (1965), Intermediate water of the Pacific Ocean, *Johns Hopkins Oceanogr. Stud., 2*, 85 pp.

Serreze M., et al. (2000), Observational evidence of recent change in the northern high-latitude environment, *Climatic Change, 46*, 159-207.

Shcherbina A. Y., L. D. Talley, D. L. Rudnick (2003), Direct observations of North Pacific ventilation: brine rejection in the Okhotsk Sea, *Science, 302*, 1952–1955.

Talley, L. D. (1991), An Okhotsk Sea water anomaly: implications for ventilation in the North Pacific, *Deep Sea Res., Part A, 38*, suppl., S171–S190.

Warner, M. J., J. L. Bullister, D. P. Wisegraver, R. H. Gammon, and R. F. Weiss (1996), Basin-wide distributions of chlorofluorocarbons CFC-11 and CFC-12 in the North Pacific, *J. Geophys. Res., 103,* 2849–2865.

Wong, A. P. S., N. L. Bindoff, and J. A. Church (1999), Large-scale freshening of intermediate waters in the Pacific and Indian Oceans, *Nature, 400*, 440–443.

Wong, C. S., R. J. Matear, H. J. Freeland, F. A. Whitney, and A. S. Bychkov (1998), WOCE line P1W in the Sea of Okhotsk: 2. CFCs and the formation rate of intermediate

water, *J. Geophys. Res., 103*, 15,625–15,642.

Yasuda, I. (1997), The origin of the North Pacific Intermediate Water, *J. Geophys. Res., 102*, 893–909.

Figure Captions

Table 1. Linear trends of potential temperature (°C/50-yr) and dissolved oxygen (ml/l/45-yr) anomaly at density 26.8–27.4 σ_θ in the Sea of Okhotsk, Oyashio, and SAC regions[a]

Figure 1. Linear trends (colors in °C/50-yr) of potential temperature anomalies at density (a) 26.8, (b) 27.0, and (c) 27.2σ_θ from 1955–2004 in the northwestern North Pacific. Large and small dots indicate grid boxes in which the linear trend is significant at the 95% and 90% confidence levels, respectively. White color indicates the grid boxes where yearly temperature anomalies are not available for more than 10 years throughout the respective periods. The significance of the linear trend estimate is based on a Student t distribution.

Figure 2. Map of acceleration potential (contours) at 27.0σ_θ relative to 2000 dbar, derived from our dataset. Boundaries of the Sea of Okhotsk (blue), Oyashio (red), and SAC regions (green), for which area-averaged quantities are displayed in Figure 3, are indicated. Shading (yellow) indicates areas where the positive linear trend of potential temperature at 27.0σ_θ exceeds the 95% confidence level.

Figure 3. Time series of (a) potential temperature (°C) and (b) dissolved oxygen (ml/l) anomalies at 27.0σ_θ averaged over the Sea of Okhotsk (blue), Oyashio (red), and SAC (green) regions, respectively (see Figure 2 for locations of these three areas). Closed circles show 5-yr averaged anomalies with errors at the 95% confidence interval for the 5-yr averages. Linear regression line for each time series is also indicated by a dashed line.

Note that in panel a (b) 0.4 °C (1.0 ml/l) and 0.8 °C (2.0 ml/l) has been added to the time series for the Oyashio and SAC regions, respectively.

Figure 4. Time series of surface air temperature anomaly in the cold season (October to March) and the linear trend over northeastern Eurasia (50°–65°N, 110°–140°E) from 1950 to 2005 (solid and dashed lines, respectively), and the annual sea ice extent anomaly in the entire Okhotsk Sea from 1979 to 2005 (blue line). The scale of the sea ice extent anomaly is indicated on the right axis and inverted. The surface air temperature anomaly is derived from *Jones* [1994], and the sea ice extent anomaly is derived from the Met Office Hadley Centre's sea ice data set [*Rayner et al.* 2003]. The surface air temperature anomaly with respect to the 27-yr average from 1979 to 2005 is shown for the benefit of comparison with the sea ice extent anomaly.

Table 1. Linear trends of potential temperature (°C/50-yr) and dissolved oxygen (ml/l/45-yr) anomaly at density 26.8–27.4 σ_θ in the Sea of Okhotsk, Oyashio, and SAC regions[a]

	Okhotsk Sea		Oyashio		SAC	
σ_θ	θ	O_2	θ	O_2	θ	O_2
26.8	**0.28**	**-0.63**	0.12	-0.34	**0.31**	-0.22
26.9	**0.66**	**-0.61**	**0.26**	**-0.53**	**0.30**	-0.13
27.0	**0.62**	**-0.58**	**0.26**	**-0.54**	**0.28**	-0.30
27.1	**0.51**	**-0.48**	**0.21**	**-0.35**	**0.18**	**-0.27**
27.2	**0.34**	**-0.41**	**0.17**	**-0.32**	**0.12**	-0.21
27.3	**0.18**	**-0.33**	**0.12**	**-0.19**	**0.06**	-0.16
27.4	**0.10**	**-0.23**	**0.07**	-0.10	0.04	-0.12

[a] Bold numbers indicate that the trend is significant at the 99% confidence level. The statistical significance is based on a Student t distribution.

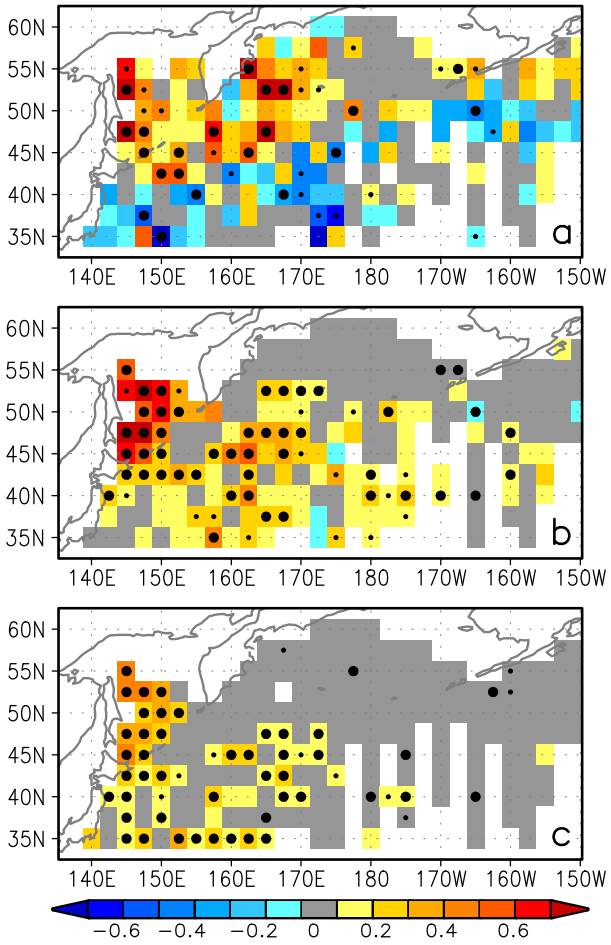

Figure 1. Linear trends (colors in °C/50-yr) of potential temperature anomalies at density (a) 26.8, (b) 27.0, and (c) 27.2σ_θ from 1955–2004 in the northwestern North Pacific. Large and small dots indicate grid boxes in which the linear trend is significant at the 95% and 90% confidence levels, respectively. White color indicates the grid boxes where yearly temperature anomalies are not available for more than 10 years throughout the respective periods. The significance of the linear trend estimate is based on a Student t distribution.

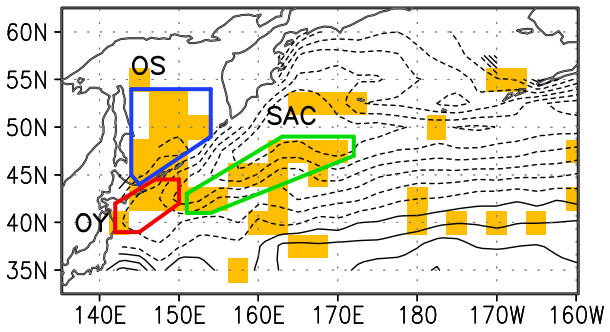

Figure 2. Map of acceleration potential (contours) at $27.0\sigma_\theta$ relative to 2000 dbar, derived from our dataset. Boundaries of the Sea of Okhotsk (blue), Oyashio (red), and SAC regions (green), for which area-averaged quantities are displayed in Figure 3, are indicated. Shading (yellow) indicates areas where the positive linear trend of potential temperature at $27.0\sigma_\theta$ exceeds the 95% confidence level.

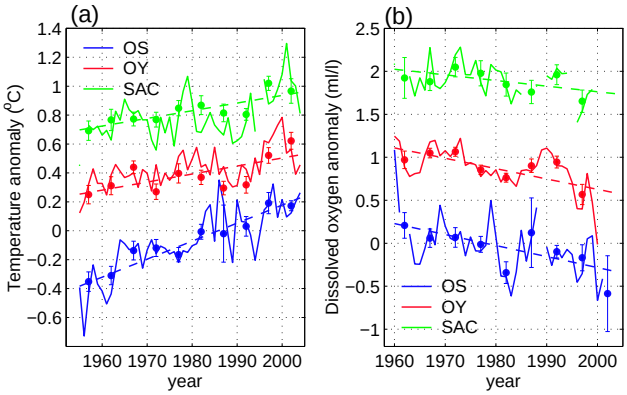

Figure 3. Time series of (a) potential temperature (°C) and (b) dissolved oxygen (ml/l) anomalies at $27.0\sigma_\theta$ averaged over the Sea of Okhotsk (blue), Oyashio (red), and SAC (green) regions, respectively (see Figure 2 for locations of these three areas). Closed circles show 5-yr averaged anomalies with errors at the 95% confidence interval for the 5-yr averages. Linear regression line for each time series is also indicated by a dashed line. Note that in panel a (b) 0.4 °C (1.0 ml/l) and 0.8 °C (2.0 ml/l) has been added to the time series for the Oyashio and SAC regions, respectively.

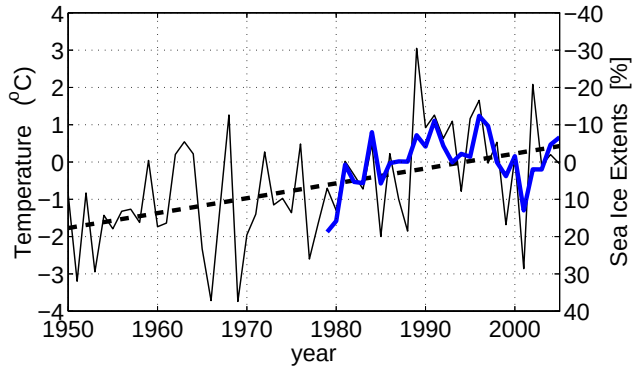

Figure 4. Time series of surface air temperature anomaly in the cold season (October to March) and the linear trend over northeastern Eurasia (50°–65°N, 110°–140°E) from 1950 to 2005 (solid and dashed lines, respectively), and the annual sea ice extent anomaly in the entire Okhotsk Sea from 1979 to 2005 (blue line). The scale of the sea ice extent anomaly is indicated on the right axis and inverted. The surface air temperature anomaly is derived from *Jones* [1994], and the sea ice extent anomaly is derived from the Met Office Hadley Centre's sea ice data set [*Rayner et al.* 2003]. The surface air temperature anomaly with respect to the 27-yr average from 1979 to 2005 is shown for the benefit of comparison with the sea ice extent anomaly.